Title

Active efflux leads to heterogeneous dissipation of proton motive force by protonophores in bacteria.

Author

Dai Le [1,2], Ekaterina Krasnopeeva [3,4,+], Faris Sinjab [3,+] , Teuta Pilizota [3,*], Minsu Kim [1,2,*]

1. Department of Physics, Emory University, Atlanta, GA, 30322. U.S.A.

2. Graduate Division of Biological and Biomedical Sciences, Emory University, Atlanta, GA, 30322. U.S.A.

3. Centre for Synthetic and Systems Biology, School of Biological Sciences, University of Edinburgh, Edinburgh, EH9 3FF, United Kingdom

4. Current Address: Institute of Science and Technology Austria, Am Campus 1, Klosterneuburg, 3400, Austria

*To whom correspondence should be addressed. Email: minsu.kim@emory.edu or teuta.pilizota@ed.ac.uk.

[+]These two authors contributed equally to this work

Abstract

Various toxic compounds disrupt bacterial physiology. While bacteria harbor defense mechanisms to mitigate the toxicity, these mechanisms are often coupled to the physiological state of the cells and become ineffective when the physiology is severely disrupted. Here, we characterized such feedback by exposing *Escherichia coli* to protonophores. Protonophores dissipate the proton motive force (PMF), a fundamental force that drives physiological functions. We found that *E. coli* cells responded to protonophores heterogeneously, resulting in bimodal distributions of cell growth, substrate transport, and

motility. Furthermore, we showed that this heterogeneous response required active efflux systems. The analysis of underlying interactions indicated the heterogeneous response results from efflux-mediated positive feedback between PMF and protonophore's action. Our studies have broad implications for bacterial adaptation to stress, including antibiotics.

Introduction

An electrochemical proton gradient across the cytoplasmic membrane, alternatively known as proton motive force (PMF), drives vital processes in cells. For example, PMF powers ATP synthesis [1,2], transport of a wide range of substrates including essential ions and metabolites [3-6], and motility [7-9]. Furthermore, PMF plays an important role in cell division [10] and cell-to-cell signaling [11,12]. Due to its importance, PMF is a key target for chemical warfare between living organisms. For example, bacteria dissipate PMF of other species to increase their colonization [13-18]. A host dissipates PMF of pathogens to slow or prevent their invasion [19,20].

One common way to dissipate PMF is via protonophores. They are a class of ionophores that collapse the proton gradient across the cell membrane by shuffling protons [21-23]. Protonophores have been extensively used in various research fields to perturb a wide range of cellular processes, particularly in the antibiotic research field due to the critical role of PMF in antibiotic influx, efflux, and mechanism of action. For example, aminoglycoside influx is PMF-driven [24], and the PMF dissipation by protonophores turns aminoglycoside from bactericidal to bacteriostatic [25] or generates antibiotic-tolerant persisters [26]. Furthermore, efflux pumps, a main culprit for multi-drug resistance, require PMF to pump antibiotic molecules out of cells [27]. Because PMF dissipation has detrimental effects on cells, protonophores themselves work as antibiotic agents [17,18,28-33]. Perhaps unsurprisingly, protonophores naturally produced by bacteria or hosts alter antibiotic efficacy [20,34,35].

The detailed action of protonophores has been extensively studied *in vitro* using reconstituted lipid-bilayer systems (e.g., [36,37]). However, *in vivo* effects of protonophores are less well understood, despite the fact that they are critical to bacterial physiology, microbial competition, host-pathogen interaction, and antibiotic action and resistance. In this study, we characterized the cellular response to protonophores.

Results

Heterogeneous responses of bacteria to protonophores.

We measured the growth of *E. coli* treated with a common protonophore, carbonyl cyanide m-chlorophenyl hydrazine (CCCP). At increasing CCCP concentrations, the rate of population growth decreased gradually (Supplementary Fig. 1A). We then monitored the growth of individual cells at 50 μM CCCP, an intermediate concentration at which a population exhibits a moderate growth reduction (Supplementary Fig. 1A). We found an all-or-none effect of CCCP at the single-cell level (Fig. 1A); some cells did not grow, whereas other cells continued to grow at the same rate as untreated cells.

We then examined how CCCP affects substrate transport by using a fluorescent dye, Hoechst 33342 (HCT) [38]. Intracellular HCT intensity was uniformly low in the absence of CCCP. At an intermediate CCCP concentrations (50 μM), we observed co-existence of cells exhibiting two distinct HCT intensities (Fig. 1B). Importantly, HCT intensity was correlated with cell growth; cells with low intensity (HCT-dim) grew unperturbed while those with high intensity (HCT-bright) exhibited no growth (Fig. 1B). Some cells transitioned from HCT-dim to HCT-bright during the experiment. After the transition, HCT-bright cells ceased to grow.

We then examined the mechanism for the co-existence of cells with the distinct cell growth and substrate transport states. Given that CCCP disrupts PMF [22], we hypothesized that the effect of CCCP on PMF is heterogeneous, i.e., it disrupts PMF severely in some cells, but not in others. To examine this hypothesis, we evaluated PMF using two different approaches. First, we used a dye sensitive to membrane potential, $DiSC_3(5)$. When extracellular pH is comparable to that of intracellular pH (as is the case for our growth

medium), membrane potential is primarily determined by PMF. $DiSC_3(5)$ accumulates in cells with strong PMF and self-quenches, resulting in low fluorescence [39,40]. We first confirmed that our working $DiSC_3(5)$ concentration (~nM) did not affect cell growth (Supplementary Fig. 1C). We then exposed cells to 50 μM CCCP and found they exhibited two distinct $DiSC_3(5)$ intensities (Fig. 1C). Because $DiSC_3(5)$ and HCT fluorescence emission spectra are well separated, they can be used simultaneously. We found that $DiSC_3(5)$-bright cells were also HCT-bright and did not grow (upper right group in Fig. 1D), whereas $DiSC_3(5)$-dim cells were HCT-dim and grew (lower left group in Fig. 1D). This observation suggests that the co-existence of cells with two distinct HCT intensities and cell growth states is caused by the heterogeneous effect of CCCP on PMF.

To further test our hypothesis, we next measured the bacterial flagellar motor speed. Flagellar motor is powered by, and its speed is proportional to, PMF [7,9]. By measuring the motor rotation speed, we previously determined a relative change in PMF [41,42]. In the absence of CCCP, the motor speed remained high and constant (Fig. 1E). Treatment with 50 μM CCCP resulted in two subpopulations, one with slightly reduced rotation (high PMF), and the other with no rotation (zero PMF); see Fig. 1F. The time point at which each cell lost PMF varied, agreeing with our observation that cell growth stopped at various times during CCCP treatment (Fig. 1B). Our observation of two distinct motor speeds and $DiSC_3(5)$ intensities in a population supports our hypothesis that CCCP disrupts the PMF of cells heterogeneously.

We then quantified the degree of heterogeneity by characterizing HCT fluorescence intensity and motor speeds over a wide range of CCCP concentrations. At low CCCP concentrations (≤ 25 μM), HCT intensity in a population was low (HCT-dim) and its distribution was unimodal; see Figs 2A-2B. The motor speed was barely affected; see Fig. 3A. An increase in the CCCP concentration to 50 μM did not shift the center of the original peak in the HCT intensity distribution but led to the appearance of another peak on the right (HCT-bright cells), showing a bimodal distribution (Fig. 2C). This agrees with the motor speed data, which showed two distinct motor speeds at this concentration (Fig. 3B). At higher

CCCP concentrations (≥ 70 μM), the original peak on the left in the HCT intensity distribution disappeared, indicating the enrichment of HCT-bright cells (Figs 2D-2E). This enrichment is accompanied by the complete collapse of PMFs, as indicated by zero motor speeds in all cells (Figs 3C-3D).

The heterogeneous effect of a protonophore is mediated by the efflux pumps.

Our observations above confirm that cells exposed to CCCP exhibit distinct PMF levels. In bacteria, positive feedback is required to stabilize distinct phenotypic states [43]. Here, we investigated a feedback mechanism that stabilizes two distinct PMF levels in a CCCP-exposed population. Bacteria can mitigate harmful effects of protonophores and other toxic compounds by extruding them with efflux pumps [44-46] (green arm in Fig. 4). But, these pumps are powered by PMF [27] (blue arm in Fig. 4) and thus are subject to disruption by protonophores (red arm in Fig. 4), suggesting an efflux-mediated positive feedback between protonophores and PMF (Fig. 4).

We experimentally tested this potential role of efflux activity by repeating our measurements using the Δ*tolC* strain. In many bacterial species including *E. coli*, TolC is a major component of efflux pumps [47], and these pumps can be inactivated by the *tolC* knock-out. We first confirmed that the *tolC* knock-out itself had little effect on the PMF level in the absence of CCCP (Supplementary Fig. 2). Our HCT measurements showed that the HCT intensity was uniform across a Δ*tolC* population, and the analysis showed the absence of a left, low-intensity peak, which results in a narrow unimodal distribution (Fig 2F). Increasing CCCP concentrations moderately shifted the peak center, but the distribution remained unimodal (Figs 2F-J), which is in contrast to a bimodal distribution in the WT strain (Figs 2A-E). This observation with the Δ*tolC* strain is consistent with motor speed measurements, which showed that Δ*tolC* cells exhibited a uniform and gradual reduction in the motor speed at increasing CCCP concentrations (Figs 3E-H). These data indicate that the efflux pumps indeed play a critical role in the heterogeneous effect of a protonophore.

We next examined the HCT intensity distribution in cells treated other common protonophores, 3,3',4',5-tetrachlorosalicylanilide (TCS) [48,49] and indole [37,41]. Similarly to CCCP, the WT cells exhibited two distinct HCT intensities in intermediate concentrations of these protonophores, and the analysis confirmed a bimodal distribution; see Supplementary Figs 3 and 4 (left panel). The centers of the two peaks were comparable to those observed in a CCCP-treated population: the left peak at ~10 A.U. and the right peak at >100 A.U. In a Δ*tolC* population, however, the HCT intensity was uniform, and the analysis showed the absence of a left, low-intensity peak (Supplementary Figs 3 and 4, right panel), which is consistent with our finding from the experiment with CCCP.

Discussion

PMF is at the basis of vital physiological functions in cells [1-11]. Protonophores are synthesized for a research purpose or produced naturally by living organisms [13-20]. For example, indole (a protonophore [37,41] tested in the present study) is one of the most abundant compounds in a dense bacterial culture and present in high concentrations in gut microbiome [12,50]. Efflux pumps transport protonophores out of cells, protecting them from protonophores' harmful effects [44,45]. The present study demonstrates that this protection is heterogeneous, protecting some cells but not all. Our findings indicate that this heterogeneity emerges because protonophores affect their own efflux transport. For example, if cells initially have a strong efflux activity, upon the exposure to protonophores, they extrude protonophores better and maintain their PMF, thereby continuing to support the strong efflux activity (opposite for cells with a weak efflux activity).

PMF has important roles in antibiotic influx, efflux, and mechanism of action. As such, protonophores were extensively used in antibiotic research. Interestingly, heterogeneous responses were observed in these studies. For example, a subpopulation of cells can tolerate antibiotics by not growing: bacterial persisters [51,52]. The post-antibiotic effect, continued growth suppression after antibiotic withdrawal, is strongly skewed by a small subpopulation that resumes growth earlier than others [53]. Protonophores have strong effects on the emergence of a persister subpopulation [26,54] and an early-grower subpopulation [55].

Importantly, these heterogeneous effects of protonophores involve efflux pumps [26,54-56]. This is consistent with our observation of heterogeneous growth phenotypes (i.e., the co-existence of non-growing and growing subpopulations), which is mediated by the feedback among protonophores, PMF, and efflux pumps. Our additional motor-speed data indicate that, upon protonophore washout, cells in the non-growing subpopulation recover their PMFs heterogeneously (Supplementary Fig. 5). We believe that our findings are useful for antibiotic research, given the important role of PMF and efflux pumps to antibiotic action and widespread use of protonophores in the field. Furthermore, some protonophores are used as antibiotic agents [17,18,28-33], for which our findings can be directly applicable.

Our results have broad implications for bacterial adaptation to stress. In natural environments, various toxic compounds negatively affect bacterial physiology. While bacteria harbor defense mechanisms to mitigate the toxicity, these mechanisms are often coupled to the physiological state of the cells and become ineffective when the physiology is severely disturbed. In our studies, this coupling is manifest as the feedback between protonophores and efflux pumps. Similar coupling could be realized through other mechanisms. For example, efflux pumps extrude biocides or other plant-derived disinfectants, but their expression is altered by these compounds, thereby forming feedback [57,58]. Cytoplasmic pH is an important determinant for antibiotic efflux [59,60] but can be altered by antibiotics [61,62]. Our studies provide insight into how such coupling could affect bacterial adaptation to these toxic compounds.

Lastly, protonophores have been extensively utilized as a powerful tool to perturb various physiological processes in cells, including cell division, motility, and antibiotic transport. It was commonly assumed that increasing protonophore concentrations lead to gradual disruption of these processes. However, our studies confirm that the disruption is heterogeneous at the single-cell level. Our data from the experiment with the Δ*tolC* strain shows that gradual disruption can be achieved but requires the inactivation of efflux activities. These results should be useful for the experimental designs and data interpretation in future studies.

Figure caption

Fig 1. Heterogeneous responses of *E. coli* to 50 μM CCCP. A) Some cells grew normally (growth rate of 0.87 ± 0.07 /hr, which is comparable to 0.83 ± 0.09 /hr for untreated cells). However, growth was completely inhibited in other cells. B) Cells exhibited two distinct HCT levels, and HCT-bright cells did not grow. Cells transitioned from HCT-dim to HCT-bright during the experiment, as indicated by HCT-bright cells in the growing micro-colony on the right. C-D) Cells exhibited two distinct intracellular $DiSC_3(5)$ intensities, which are correlated with HCT intensities. The scale bar represents 5 μm. Note that HCT intensities were quantified in Fig. 2, which showed the HCT intensity distribution differs between the Δ*tolC* and WT strains. We thus compared the $DiSC_3(5)$ intensity in the Δ*tolC* and WT strains. We found that $DiSC_3(5)$ intensity in the Δ*tolC* strain was moderately higher (~50%). While this finding agrees with the previous finding that $DiSC_3(5)$ is a substrate of the efflux pumps [63], the efflux activity is only moderate and cannot explain the 10-fold difference in $DiSC_3(5)$ intensity between $DiSC_3(5)$-bright and $DiSC_3(5)$-weak cells in Fig. 1D. E). In the absence of CCCP, the motor speeds were uniform across a population. F). When exposed to CCCP, cells exhibited two distinct motor speeds.

Fig 2. HCT fluorescence intensity distribution in cells treated with various CCCP concentrations. A-B) At low CCCP concentrations (≤ 25 μM), HCT intensity was low across a population (HCT-dim), resulting in a unimodal distribution with the peak center near ~10 A.U. C) Increasing the CCCP concentration to 50 μM did not shift the peak center but led to the appearance of another peak on the right (> 100 A.U.), showing a bimodal distribution. At higher (≥ 75 μM) CCCP concentrations, the left low-intensity peak disappeared, showing the enrichment of HCT-bright cells. F-J). The Δ*tolC* strain lacks a peak on the left, exhibiting a unimodal distribution. More than 200 cells were analyzed for each condition. We made a similar observation for two other protonophores, TCS and indole (Supplementary Figs 3 and 4).

Fig 3. Flagellar motor speeds of cells treated with various CCCP concentrations. A) At low CCCP concentrations, the motor speeds of WT cells were barely affected. B) Cells exhibited two distinct motor

speeds at 50 μM CCCP, one with a slightly reduced rotation (high PMF), and the other with no rotation (zero PMF). C-D) At higher CCCP concentrations (≥ 70 μM), the motor speeds were zero in all cells. E-H) The Δ*tolC* strain exhibited a uniform and gradual reduction in the motor speed at increasing CCCP concentrations. Note that, at very low PMF values where the bacterial flagellar motor operates with one stator unit, the motor can transiently stop in a step-like manner [64,65], which can explain the purple trajectory in Fig. 3F. Motor speed measurements are laborious and time-consuming. The motor speeds of 10~15 cells were analyzed for each condition except for the experiment with the WT strain exposed to 100 μM CCCP (where 4 cells were analyzed).

Fig 4. Model of efflux-mediated positive feedback. Efflux pumps transport protonophores out of cells [44,45] (green arm). The pump is powered by PMF [27] (blue arm) and thus is subject to disruption by protonophores (red arm).

Materials and Methods

Bacterial strains and growth conditions

E. coli K-12 NCM3722 [66-68] and Neidhart's MOPS minimal media [69] with glucose and ammonium as the carbon and nitrogen sources were used, except the motor speed measurement (see below). See Supplementary Table 1 for all the ingredients and their concentrations used in the media. The media pH is 7.0, which allowed *E. coli* to keep neutral cytoplasmic pH and ensured HCT fluorescence does not incur any pH-related intensity changes [70]. To make the Δ*tolC* strain (NMK320), the *tolC* gene deletion allele from the Keio deletion collection [71,72] was transferred to the NCM3722 strain using P1 transduction [73]. The Km^r gene was flipped out as previously described [71,72]. Cells were cultured at 37°C with constant agitation at 250 rpm in a water bath (New Brunswick Scientific). To monitor their growth, the optical density (OD_{600}) of the culture was measured using a Genesys20 spectrophotometer (Thermo-Fisher) with a standard cuvette (16.100-Q-10/Z8.5, Starna Cells Inc). See Supplementary Methods for details.

Fluorescence microscopy

At the OD_{600} of ~0.1, cells were loaded onto No. 1.5 cover-glasses. 1 mm-thick 1.5% agarose pads, made with the same MOPS growth media (containing the same concentrations of HCT, $DiSC_3(5)$ and/or protonophores), were used to cover the cells. Cells were imaged with a pre-warmed (at 37°C) inverted microscope (Olympus IX83 P2Z) with Neo 5.5 sCMOS camera (Andor Neo). Intracellular HCT and $DiSC_3(5)$ were imaged using DAPI and Cy5 fluorescence filter sets. Images were acquired with MetaMorph Microscopy Automation and Image Analysis Software, and analyzed with MicrobeJ 5.13m_4 plug-in in ImageJ [74]. MicrobeJ can automatically segment cell boundaries from phase-contrast microscope images and apply the binary masks from the segmentation to measure fluorescence intensities inside and outside the cells. The latter (background) is subtracted from the former to determine intracellular fluorescence signals.

Motor speed measurement

E. coli K-12 MG1655 with genetically modified flagellar filaments (EK07 [41]) was used. It was cultured in Lysogeny broth (LB) (10 g tryptone, 5 g yeast extract, 10 g NaCl per 1 L) to the OD_{600} of ~2. Cells were sheared to truncate flagellar filaments, washed from LB to modified minimal medium (MM9: 50 mM Na_2HPO_4, 25 mM NaH_2PO_4, 8.5 mM NaCl, 18.7 mM NH_4Cl, 0.1 mM $CaCl_2$, 1 mM KCl, 2 mM $MgSO_4$) supplemented with 0.3% D-glucose, and attached to the cover glass surface of a tunnel slide via poly-L-lysine [41,75,76]. 0.5 μm polystyrene beads were attached to truncated flagellar filaments and placed into the focus of a heavily attenuated optical trap (855 nm laser) to detect the motor rotation [41]. Time course of the bead rotation was recorded with the position-sensitive detector (Model 2931; New Focus, Irvine, CA) at 10 kHz, and a 2.5 kHz cutoff antialiasing filter applied before processing the signal. Next, a flat-top window discrete Fourier transform (window size = 16,384 data points with a step dt = 0.01 s) was applied to the acquired x and y coordinates of a bead position to obtain a time series motor speed recording. The speed traces were then median-filtered with a 401-point moving window, after manual removal of spurious zeroes caused by flowing CCCP/media into the slide. The filtered speed trace was then

resampled to 10 samples/minute for plotting. Measurements were made with a microscope equipped with back focal-plane interferometry capability[77,78], as described previously [77-79].

Reference

1. Maloney PC, Kashket ER, Wilson TH. *A protonmotive force drives ATP synthesis in bacteria*. Proceedings of the National Academy of Sciences of the United States of America. 1974;71(10):3896-900.

2. Mitchell P. *Chemiosmotic coupling in oxidative and photosynthetic phosphorylation*. Biological Reviews. 1966;41(3):445-501.

3. Harold FM, Van Brunt J. *Circulation of H+ and K+ across the plasma membrane is not obligatory for bacterial growth*. Science. 1977;197(4301):372-3.

4. Ohsumi Y, Anraku Y. *Active transport of basic amino acids driven by a proton motive force in vacuolar membrane vesicles of Saccharomyces cerevisiae*. The Journal of biological chemistry. 1981;256(5):2079-82.

5. Nelson N. *Energizing porters by proton-motive force*. Journal of Experimental Biology. 1994;196(1):7-13.

6. Kim BH, Gadd GM. Membrane transport – nutrient uptake and protein excretion. Prokaryotic Metabolism and Physiology. 2 ed. Cambridge: Cambridge University Press; 2019. p. 31-57.

7. Fung DC, Berg HC. *Powering the flagellar motor of Escherichia coli with an external voltage source*. Nature. 1995;375(6534):809-12.

8. Manson MD, Tedesco P, Berg HC, Harold FM, Van der Drift C. *A protonmotive force drives bacterial flagella*. Proceedings of the National Academy of Sciences. 1977;74(7):3060-4.

9. Gabel CV, Berg HC. *The speed of the flagellar rotary motor of Escherichia coli varies linearly with protonmotive force*. Proceedings of the National Academy of Sciences. 2003;100(15):8748-51.

10. Strahl H, Hamoen LW. *Membrane potential is important for bacterial cell division*. Proceedings of the National Academy of Sciences of the United States of America. 2010;107(27):12281-6.

11. Prindle A, Liu J, Asally M, Ly S, Garcia-Ojalvo J, Süel GM. *Ion channels enable electrical communication in bacterial communities*. Nature. 2015;527(7576):59-63.

12. Lee J-H, Lee J. *Indole as an intercellular signal in microbial communities*. FEMS microbiology reviews. 2010;34(4):426-44.

13. van Belkum MJ, Kok J, Venema G, Holo H, Nes IF, Konings WN, Abee T. *The bacteriocin lactococcin A specifically increases permeability of lactococcal cytoplasmic membranes in a voltage-independent, protein-mediated manner*. J Bacteriol. 1991;173(24):7934-41.

14. Gao FH, Abee T, Konings WN. *Mechanism of action of the peptide antibiotic nisin in liposomes and cytochrome c oxidase-containing proteoliposomes*. Applied and environmental microbiology. 1991;57(8):2164-70.

15. Montville TJ, Bruno MEC. *Evidence that dissipation of proton motive force is a common mechanism of action for bacteriocins and other antimicrobial proteins*. International journal of food microbiology. 1994;24(1):53-74.

16. Lamsa A, Liu W-T, Dorrestein PC, Pogliano K. *The Bacillus subtilis cannibalism toxin SDP collapses the proton motive force and induces autolysis*. Molecular microbiology. 2012;84(3):486-500.

17. Bruno ME, Kaiser A, Montville TJ. *Depletion of proton motive force by nisin in Listeria monocytogenes cells*. Applied and environmental microbiology. 1992;58(7):2255-9.

18. Venema K, Abee T, Haandrikman AJ, Leenhouts KJ, Kok J, Konings WN, Venema G. *Mode of Action of Lactococcin B, a Thiol-Activated Bacteriocin from Lactococcus lactis*. Applied and environmental microbiology. 1993;59(4):1041-8.

19. Dankert JR, Esser AF. *Bacterial killing by complement. C9-mediated killing in the absence of C5b-8*. The Biochemical journal. 1987;244(2):393-9.

20. McCollister BD, Hoffman M, Husain M, Vázquez-Torres A. *Nitric oxide protects bacteria from aminoglycosides by blocking the energy-dependent phases of drug uptake*. Antimicrob Agents Chemother. 2011;55(5):2189-96.

21. Mitchell P. *Chemiosmotic coupling in oxidative and photosynthetic phosphorylation*. Biochimica et Biophysica Acta (BBA) - Bioenergetics. 2011;1807(12):1507-38.

22. Kasianowicz J, Benz R, McLaughlin S. *The kinetic mechanism by which CCCP (carbonyl cyanidem-Chlorophenylhydrazone) transports protons across membranes*. The Journal of Membrane Biology. 1984;82(2):179-90.

23. McLaughlin SG, Dilger JP. *Transport of protons across membranes by weak acids*. Physiological Reviews. 1980;60(3):825-63.

24. Taber HW, Mueller JP, Miller PF, Arrow AS. *Bacterial uptake of aminoglycoside antibiotics*. Microbiological reviews. 1987;51(4):439-57.

25. Bruni GN, Kralj JM. *Membrane voltage dysregulation driven by metabolic dysfunction underlies bactericidal activity of aminoglycosides*. eLife. 2020;9:e58706.

26. Allison KR, Brynildsen MP, Collins JJ. *Metabolite-enabled eradication of bacterial persisters by aminoglycosides*. Nature. 2011;473(7346):216-20.

27. Paulsen IT, Brown MH, Skurray RA. *Proton-dependent multidrug efflux systems*. Microbiological reviews. 1996;60(4):575-608.

28. Aowicki D, Huczyński A. *Structure and antimicrobial properties of monensin A and its derivatives: summary of the achievements*. Biomed Res Int. 2013;2013:742149-.

29. Farha MA, Verschoor CP, Bowdish D, Brown ED. *Collapsing the proton motive force to identify synergistic combinations against Staphylococcus aureus*. Chem Biol. 2013;20(9):1168-78.

30. Ahmed S, Booth IR. *The use of valinomycin, nigericin and trichlorocarbanilide in control of the protonmotive force in Escherichia coli cells*. The Biochemical journal. 1983;212(1):105-12.

31. Feng X, Zhu W, Schurig-Briccio LA, Lindert S, Shoen C, Hitchings R, Li J, Wang Y, Baig N, Zhou T, Kim BK, Crick DC, Cynamon M, McCammon JA, Gennis RB, Oldfield E. *Antiinfectives targeting enzymes and the proton motive force*. Proceedings of the National Academy of Sciences. 2015;112(51):E7073-E82.

32. Jeon AB, Ackart DF, Li W, Jackson M, Melander RJ, Melander C, Abramovitch RB, Chicco AJ, Basaraba RJ, Obregón-Henao A. *2-aminoimidazoles collapse mycobacterial proton motive force and block the electron transport chain*. Scientific reports. 2019;9(1):1513.

33. Valderrama K, Pradel E, Firsov AM, Drobecq H, Bauderlique-le Roy H, Villemagne B, Antonenko YN, Hartkoorn RC. *Pyrrolomycins Are Potent Natural Protonophores*. Antimicrob Agents Chemother. 2019;63(10):e01450-19.

34. Vega NM, Allison KR, Khalil AS, Collins JJ. *Signaling-mediated bacterial persister formation*. Nat Chem Biol. 2012;8(5):431-3.

35. Crabbé A, Ostyn L, Staelens S, Rigauts C, Risseeuw M, Dhaenens M, Daled S, Van Acker H, Deforce D, Van Calenbergh S, Coenye T. *Host metabolites stimulate the bacterial proton motive force to enhance the activity of aminoglycoside antibiotics*. PLoS pathogens. 2019;15(4):e1007697.

36. Leblanc OH, Jr. *The effect of uncouplers of oxidative phosphorylation on lipid bilayer membranes: Carbonylcyanidem-chlorophenylhydrazone*. J Membr Biol. 1971;4(1):227-51.

37. Chimerel C, Field CM, Piñero-Fernandez S, Keyser UF, Summers DK. *Indole prevents Escherichia coli cell division by modulating membrane potential*. Biochimica et biophysica acta. 2012;1818(7):1590-4.

38. van den Berg van Saparoea HB, Lubelski J, van Merkerk R, Mazurkiewicz PS, Driessen AJ. *Proton motive force-dependent Hoechst 33342 transport by the ABC transporter LmrA of Lactococcus lactis*. Biochemistry. 2005;44(51):16931-8.

39. Te Winkel JD, Gray DA, Seistrup KH, Hamoen LW, Strahl H. *Analysis of Antimicrobial-Triggered Membrane Depolarization Using Voltage Sensitive Dyes*. Front Cell Dev Biol. 2016;4:29-.

40. Síp M, Herman P, Plásek J, Hrouda V. *Transmembrane potential measurement with carbocyanine dye diS-C3-(5): fast fluorescence decay studies*. Journal of photochemistry and photobiology B, Biology. 1990;4(3):321-8.

41. Krasnopeeva E, Lo C-J, Pilizota T. *Single-Cell Bacterial Electrophysiology Reveals Mechanisms of Stress-Induced Damage*. Biophysical journal. 2019;116(12):2390-9.

42. Mancini L, Terradot G, Tian T, Pu Y, Li Y, Lo C-J, Bai F, Pilizota T. *A General Workflow for Characterization of Nernstian Dyes and Their Effects on Bacterial Physiology*. Biophysical journal. 2020;118(1):4-14.

43. Mitrophanov AY, Groisman EA. *Positive feedback in cellular control systems*. BioEssays. 2008;30(6):542-55.

44. Lomovskaya O, Lewis K. *Emr, an Escherichia coli locus for multidrug resistance*. Proceedings of the National Academy of Sciences of the United States of America. 1992;89(19):8938-42.

45. Nikaido H. *Multidrug efflux pumps of gram-negative bacteria*. J Bacteriol. 1996;178(20):5853-9.

46. Griffith JM, Basting PJ, Bischof KM, Wrona EP, Kunka KS, Tancredi AC, Moore JP, Hyman MRL, Slonczewski JL. *Experimental Evolution of Escherichia coli K-12 in the Presence of Proton*

354 *Motive Force (PMF) Uncoupler Carbonyl Cyanide m-Chlorophenylhydrazone Selects for Mutations*
355 *Affecting PMF-Driven Drug Efflux Pumps*. Applied and environmental microbiology.
356 2019;85(5):e02792-18.

357 47. Du D, Wang-Kan X, Neuberger A, van Veen HW, Pos KM, Piddock LJV, Luisi BF. *Multidrug*
358 *efflux pumps: structure, function and regulation*. Nature Reviews Microbiology. 2018;16(9):523-39.

359 48. MacLeod RA, Wisse GA, Stejskal FL. *Sensitivity of some marine bacteria, a moderate halophile,*
360 *and Escherichia coli to uncouplers at alkaline pH*. J Bacteriol. 1988;170(9):4330-7.

361 49. Feng X-C, Guo W-Q, Zheng H-S, Wu Q-L, Luo H-C, Ren N-Q. *Effect of metabolic uncoupler,*
362 *3,3′,4′,5-tetrachlorosalicylanilide (TCS) on Bacillus subtilis: biofilm formation, flocculability and surface*
363 *characteristics*. RSC Adv. 2018;8(29):16178-86.

364 50. Berstad A, Raa J, Valeur J. *Indole - the scent of a healthy 'inner soil'*. Microb Ecol Health Dis.
365 2015;26:27997-.

366 51. Balaban NQ, Merrin J, Chait R, Kowalik L, Leibler S. *Bacterial persistence as a phenotypic*
367 *switch*. Science. 2004;305(5690):1622-5.

368 52. Şimşek E, Kim M. *Power-law tail in lag time distribution underlies bacterial persistence*.
369 Proceedings of the National Academy of Sciences. 2019;116(36):17635-40.

370 53. MacKenzie FM, Gould IM. *The post-antibiotic effect*. J Antimicrob Chemother. 1993;32(4):519-
371 37.

372 54. Kwan BW, Valenta JA, Benedik MJ, Wood TK. *Arrested Protein Synthesis Increases Persister-*
373 *Like Cell Formation*. Antimicrob Agents Chemother. 2013;57(3):1468-73.

374 55. Srimani JK, Huang S, Lopatkin AJ, You L. *Drug detoxification dynamics explain the*
375 *postantibiotic effect*. Mol Syst Biol. 2017;13(10):948-.

56. Pu Y, Zhao Z, Li Y, Zou J, Ma Q, Zhao Y, Ke Y, Zhu Y, Chen H, Baker Matthew AB, Ge H, Sun Y, Xie Xiaoliang S, Bai F. *Enhanced Efflux Activity Facilitates Drug Tolerance in Dormant Bacterial Cells*. Mol Cell. 2016;62(2):284-94.

57. Blanco P, Hernando-Amado S, Reales-Calderon JA, Corona F, Lira F, Alcalde-Rico M, Bernardini A, Sanchez MB, Martinez JL. *Bacterial Multidrug Efflux Pumps: Much More Than Antibiotic Resistance Determinants*. Microorganisms. 2016;4(1):14.

58. Alcalde-Rico M, Hernando-Amado S, Blanco P, Martínez JL. *Multidrug Efflux Pumps at the Crossroad between Antibiotic Resistance and Bacterial Virulence*. Frontiers in Microbiology. 2016;7(1483).

59. Martins A, Spengler G, Rodrigues L, Viveiros M, Ramos J, Martins M, Couto I, Fanning S, Pagès J-M, Bolla JM, Molnar J, Amaral L. *pH Modulation of efflux pump activity of multi-drug resistant Escherichia coli: protection during its passage and eventual colonization of the colon*. PloS one. 2009;4(8):e6656-e.

60. Amaral L, Fanning S, Pagès JM. Efflux Pumps of Gram-Negative Bacteria: Genetic Responses to Stress and the Modulation of their Activity by pH, Inhibitors, and Phenothiazines. Advances in Enzymology and Related Areas of Molecular Biology2011. p. 61-108.

61. Nicholls DG, Ferguson SJ. Ion transport across energy-conserving membranes. Bioenergetics: Academic Press; 1992. p. 22-37.

62. Hards K, McMillan DGG, Schurig-Briccio LA, Gennis RB, Lill H, Bald D, Cook GM. *Ionophoric effects of the antitubercular drug bedaquiline*. Proceedings of the National Academy of Sciences. 2018;115(28):7326-31.

63. Salcedo-Sora JE, Jindal S, apos, Hagan S, Kell DB. *A palette of fluorophores that are differentially accumulated by wild-type and mutant strains of Escherichia coli: surrogate ligands for profiling bacterial membrane transporters*. Microbiology. 2021.

64. Leake MC, Chandler JH, Wadhams GH, Bai F, Berry RM, Armitage JP. *Stoichiometry and turnover in single, functioning membrane protein complexes*. Nature. 2006;443(7109):355-8.

65. Wadhwa N, Phillips R, Berg HC. *Torque-dependent remodeling of the bacterial flagellar motor*. Proceedings of the National Academy of Sciences. 2019;116(24):11764-9.

66. Soupene E, van Heeswijk WC, Plumbridge J, Stewart V, Bertenthal D, Lee H, Prasad G, Paliy O, Charernnoppakul P, Kustu S. *Physiological studies of Escherichia coli strain MG1655: Growth defects and apparent cross-regulation of gene expression*. J Bacteriol. 2003;185(18):5611-26.

67. Lyons E, Freeling M, Kustu S, Inwood W. *Using Genomic Sequencing for Classical Genetics in E. coli K12*. PloS one. 2011;6(2):e16717.

68. Brown SD, Jun S. *Complete Genome Sequence of Escherichia coli NCM3722*. Genome Announcements. 2015;3(4).

69. Neidhardt FC, Bloch PL, Smith DF. *Culture medium for enterobacteria*. J Bacteriol. 1974;119(3):736-47.

70. Swain BM, Guo D, Singh H, Rawlins PB, McAlister M, van Veen HW. *Complexities of a protonatable substrate in measurements of Hoechst 33342 transport by multidrug transporter LmrP*. Scientific reports. 2020;10(1):20026.

71. Baba T, Ara T, Hasegawa M, Takai Y, Okumura Y, Baba M, Datsenko KA, Tomita M, Wanner BL, Mori H. *Construction of Escherichia coli K-12 in-frame, single-gene knockout mutants: the Keio collection*. Mol Syst Biol. 2006;2:2006 0008.

72. Datsenko KA, Wanner BL. *One-step inactivation of chromosomal genes in Escherichia coli K-12 using PCR products*. Proceedings of the National Academy of Sciences. 2000;97(12):6640-5.

73. Thomason LC, Costantino N, Court DL. *E. coli genome manipulation by P1 transduction*. Current protocols in molecular biology / edited by Frederick M Ausubel [et al]. 2007;Chapter 1:Unit 1 17.

74. Ducret A, Quardokus EM, Brun YV. *MicrobeJ, a tool for high throughput bacterial cell detection and quantitative analysis*. Nature Microbiology. 2016;1:16077.

75. Wang Y-K, Krasnopeeva E, Lin S-Y, Bai F, Pilizota T, Lo C-J. *Comparison of Escherichia coli surface attachment methods for single-cell microscopy*. Scientific reports. 2019;9(1):19418.

76. Krasnopeeva E, Barboza-Perez UE, Rosko J, Pilizota T, Lo CJ. *Bacterial flagellar motor as a multimodal biosensor*. Methods. 2020.

77. Denk W, Webb WW. *Optical measurement of picometer displacements of transparent microscopic objects*. Appl Opt. 1990;29(16):2382-91.

78. Svoboda K, Schmidt CF, Schnapp BJ, Block SM. *Direct observation of kinesin stepping by optical trapping interferometry*. Nature. 1993;365(6448):721-7.

79. Rosko J, Martinez VA, Poon WCK, Pilizota T. *Osmotaxis in Escherichia coli through changes in motor speed*. Proceedings of the National Academy of Sciences. 2017;114(38):E7969-E76.

Fig. 1

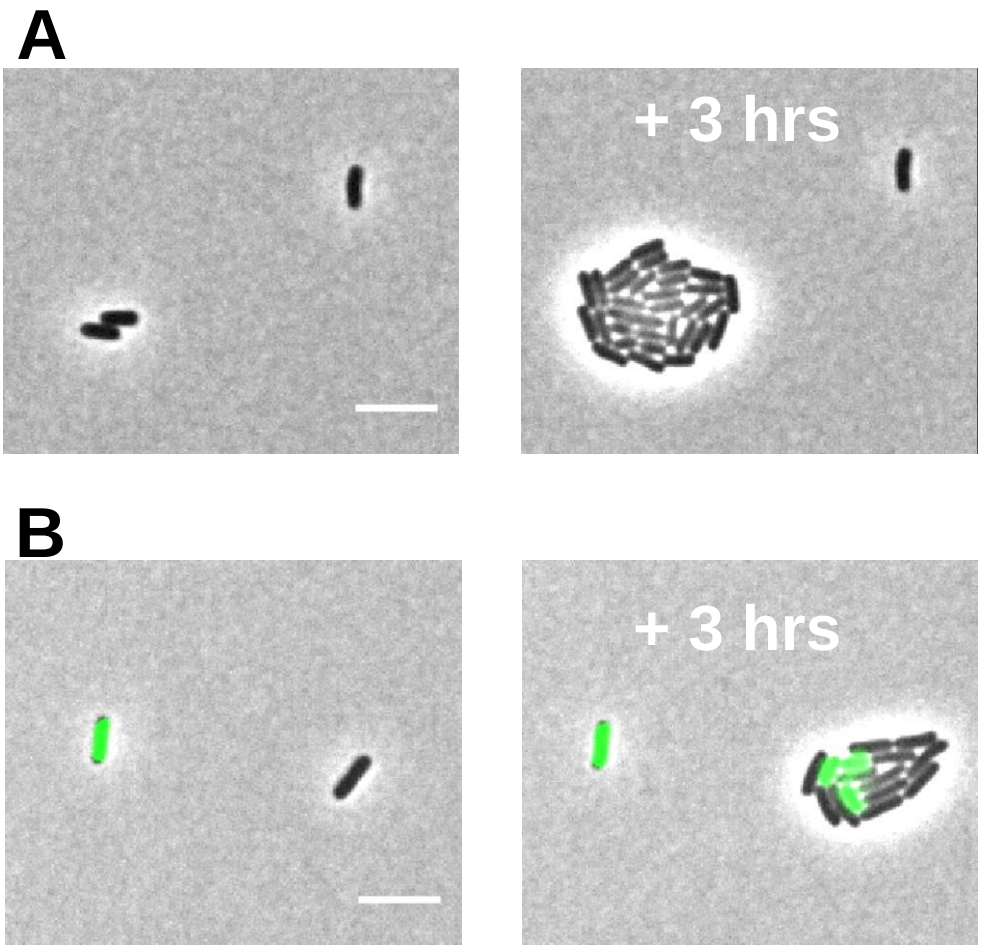
A
+ 3 hrs
B
+ 3 hrs
C
D
DiSC3(5) intensity (A.U.)
1000
100
1
10
100
1000
HCT intensity (A.U.)
E
Motor Speed (Hz)
200
100
0
0
5
10
Time (min)
F
50 μM CCCP
Motor Speed (Hz)
200
100
0
0
5
10
Time (min)

Fig. 2

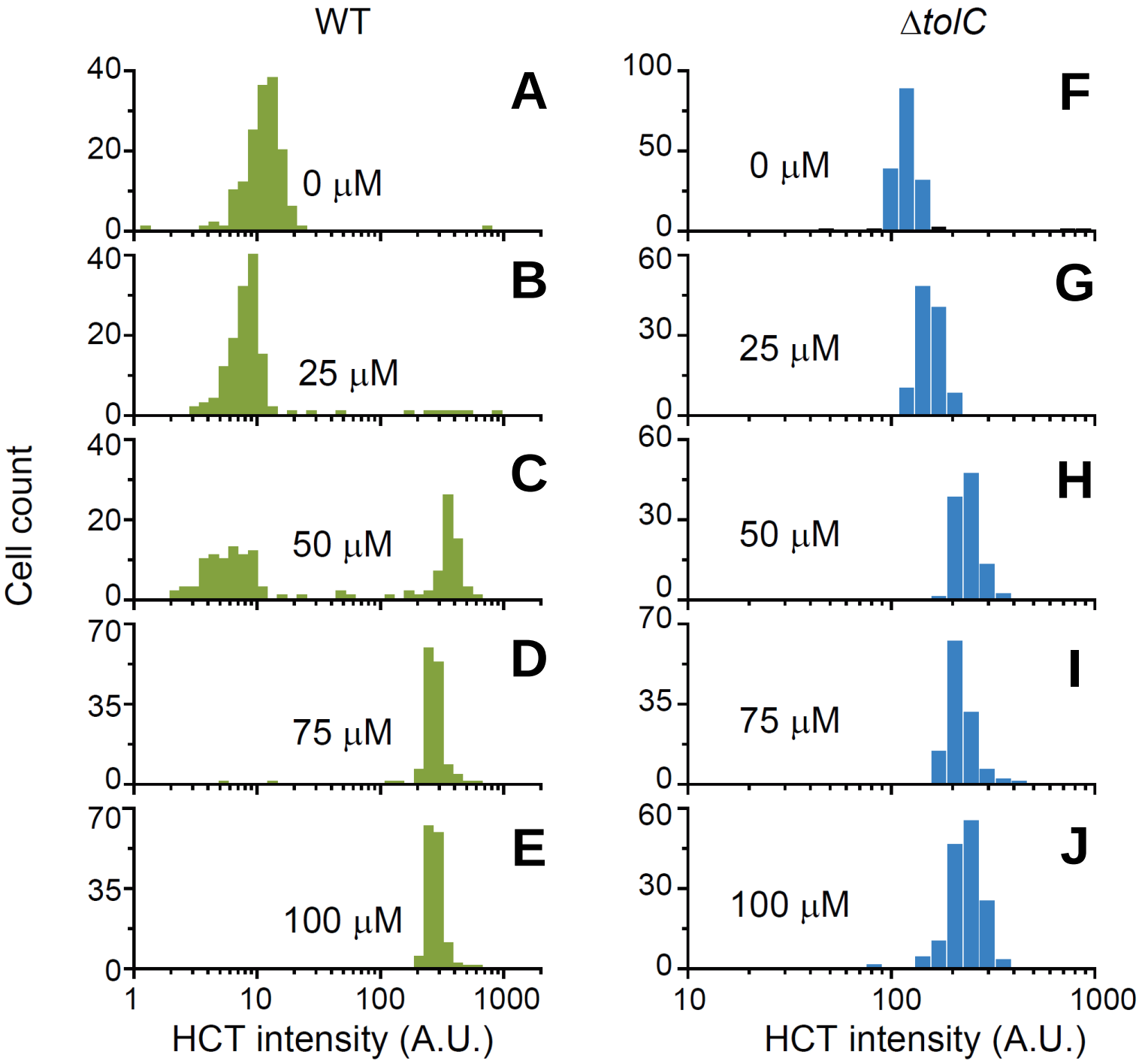
WT
ΔtolC
A
B
C
D
E
F
G
H
I
J
0 μM
25 μM
50 μM
75 μM
100 μM
Cell count
HCT intensity (A.U.)
HCT intensity (A.U.)

Fig. 3

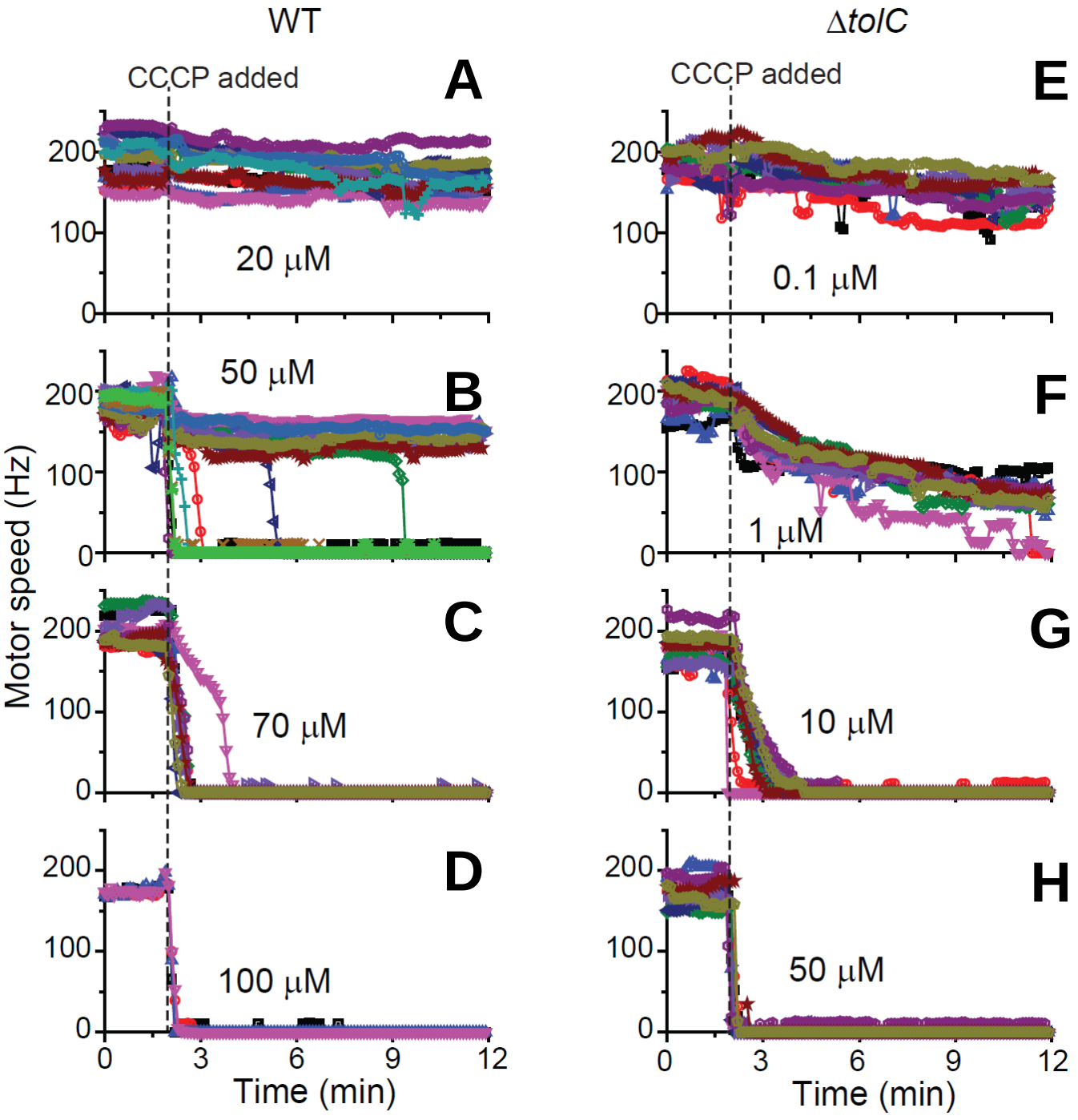
WT
ΔtolC
CCCP added
CCCP added
A
B
C
D
E
F
G
H
20 μM
50 μM
70 μM
100 μM
0.1 μM
1 μM
10 μM
50 μM
Motor speed (Hz)
Time (min)
Time (min)
0
100
200
0
3
6
9
12

Fig. 4